Int J Theor Phys (2008) 47: 3035–3056
DOI 10.1007/s10773-008-9738-6

Even and Odd Nonlinear Negative Binomial States

M. Darwish

Received: 5 December 2007 / Accepted: 4 April 2008 / Published online: 17 April 2008

Abstract In this paper the even and odd nonlinear negative binomial states of the radiation field are introduced. These states interpolates between even (odd) number states and the even (odd) nonlinear coherent states. The Glauber second-order correlation function is calculated for these states. The squeezing phenomenon (normal and amplitude-squared squeezing), the quasi-probability distribution function Q-function, Wigner-function and the phase properties, are also discussed. Examination of the resonance fluorescence against the present state is given. It has been shown that the atomic inversion is sensitive to any variation in the even and odd nonlinear negative binomial number M and the nonlinearity parameter η.

Keywords Even and add nonlinear negative binomial states · The Glauber second order correlation function · The squeezing · The quasi-probability distribution function

1 Introduction

The Fock number state $|n\rangle$ is an eigenstate of the photon number operator $\hat{n} = \hat{a}^{\dagger}\hat{a}$. Any generalization of any pure photon state of quantized radiation field is expressed as a linear combination of this state. As an example, consider the coherent state which is an eigenfunction of the annihilation operator $\hat{a}$, it can be expressed as a linear combination of all $|n\rangle$ states with coefficients chosen such that the photon counting distribution is Poissonian. These two states have been extensively studied since the early days of quantum mechanics [1, 2].

Recently there has been considerable interest in generating and producing new quantum states in addition to the number state and the coherent state. As some examples one can find: binomial state (BS) [3] (interpolating between the number state and the coherent state), negative binomial state (NBS) [4–6] (in limiting cases it gives the coherent state and the

M. Darwish (✉)
Department of Physics, Faculty of Education, Suez Canal University at Al-Arish, Al-Arish, Egypt
e-mail: motaz_darwish@yahoo.com

Present address:
M. Darwish
Department of Physics, Teachers Colleges Makkah, Umm-Alqura University, Umm-Alqura, SA

pure thermal state), logarithmic state [7] (it is a special case of NBS), generalized geometric state [8] (interpolating between the pure number states and the pure chaotic state), even BS [9] (interpolating between the even number state and the even coherent state), excited binomial states (EBS) and excited negative binomial states (ENBS) [10] (in different limits they reduce to Fock states and displaced Fock states). For a recent review of intermediate states, we may refer to [11, 12]. Recent advances in the field of trapped ions make it possible to produce intermediate states at well [13].

On the other hand, nonlinear coherent states [14, 15] are coherent states corresponding to nonlinear algebras rather than Lie algebras. The notion of nonlinear coherent states has been generalized to the even and odd nonlinear coherent states [16, 17] and it was found that these states have rather different statistical properties from those of the usual even and odd coherent states.

The nonlinear binomial state, which interpolates between the nonlinear coherent and number state was introduced with a generation scheme for the state [18]. In addition, the nonlinear negative binomial state was introduced and some of its properties have been discussed [19].

In the present work, we introduce the even and odd nonlinear negative binomial states of the radiation field as superposition of a pair of nonlinear NBS. These states can give as limiting cases the even (odd) nonlinear coherent states. Therefore, we shall devote the next section to introducing both even nonlinear negative binomial state (ENLNBS) and odd nonlinear negative binomial state (ONLNBS) and discuss some of their nonclassical properties. In Sect. 3 we study the Glauber second-order correlation function, normal and amplitude-squared squeezing, the quasi-probability distribution functions (Q-function and Wigner function) and the phase probability distribution function. While in Sect. 4 as an application we examined the behavior of the resonance fluorescence for the present states. Finally, the conclusions are summed up in Sect. 5.

2 ENLNBS and ONLNBS

Let us remind ourselves with the nonlinear negative binomial state which is defined by [19]

$$|M,\xi\rangle = \lambda \sum_{n=0}^{\infty} \binom{M+n}{n}^{\frac{1}{2}} \xi^n (f(n))!|n\rangle \tag{1}$$

where the nonlinearity function $f(n)! = \prod_{i=0}^{n} f(i)$ and $f(0) = 1$, ξ is generally complex with $0 \leq |\xi| \leq 1$, and λ is the normalization constant given by

$$|\lambda|^{-2} = \sum_{n=0}^{\infty} \binom{M+n}{n} |\xi|^{2n} [(f(n))!]^2 \tag{2}$$

One can introduce the ENLNBS as the form

$$|M,\xi\rangle_e = \lambda_e \sum_{n=0}^{\infty} \binom{M+2n}{2n}^{\frac{1}{2}} \xi^{2n} (f(2n))!|2n\rangle \tag{3}$$

and

$$|\lambda_e|^{-2} = \sum_{n=0}^{\infty} \binom{M+2n}{2n} |\xi|^{2(2n)} [(f(2n))!]^2 \tag{4}$$

And the ONLNBS as the form

$$|M,\xi\rangle_o = \lambda_o \sum_{n=0}^{\infty} \binom{M+2n+1}{2n+1}^{\frac{1}{2}} \xi^{2n+1} (f(2n+1))! |2n+1\rangle \tag{5}$$

where

$$|\lambda_o|^{-2} = \sum_{n=0}^{\infty} \binom{M+2n+1}{2n+1} \xi^{2(2n+1)} [(f(2n+1))!]^2 \tag{6}$$

These states are superposition of the two nonlinear negative binomial states $|M,\xi\rangle$ and $|M,-\xi\rangle$. As a matter of fact $|M,\xi\rangle_e \propto (|M,\xi\rangle + |M,-\xi\rangle)$ and $|M,\xi\rangle_o \propto (|M,\xi\rangle - |M,-\xi\rangle)$. The ENLBS (ONLBS) are states composed of even (odd) Fock state only. In what follows we consider some of the properties of these states.

3 Non-classical Properties

In this section we shall study the non-classical properties of the ENLNBS and ONLNBS. In the present work the nonlinearity function will be taken as two forms, the first form is $f(\hat{n}) = \frac{1}{\sqrt{n}}$ and $f(0) = 1$ [20–22]. A choice of this type appears in a natural way in Hamiltonians describing interaction with intensity-dependent coupling between a two level atom and the electromagnetic field [23–27]. While the second form is [28–31]:

$$f(n) = L_n^1(\eta^2)[(n+1)L_n^0(\eta^2)]^{-1} \tag{7}$$

with

$$L_n^k(x) = \sum_{m=0}^{n} (-1)^m \frac{(n+k)!x^m}{(n-m)!(k+m)!m!} \tag{8}$$

where $L_n^k(x)$ are the associated Laguerre polynomials and η is known as the Lamb-Dicke parameter. This function (7) appears in the study of the quantized motion of the center of mass of trapped ions [32, 33]. Clearly, $f(n) = 1$ when $\eta = 0$ and in this case NLNBS become the NBS. However, when $\eta \neq 0$ nonlinearity starts developing, with the degree of nonlinearity depending on the magnitude of η [32].

3.1 Photon Statistics

One calculates the mean of power of photon number $\bar{n}$, which is the expectation value of the number operator $\hat{n} = \hat{a}^\dagger \hat{a}$ in ENLNBS of (3).

$$\langle \hat{n^r} \rangle_e = |\lambda_e|^2 \sum_{n=0}^{\infty} \binom{M+2n}{2n} \xi^{2n} [f(2n)!]^2 (2n)^r \tag{9}$$

While the expectation value of ONLNBS of (5) is given by

$$\langle \hat{n^r} \rangle_o = |\lambda_o|^2 \sum_{n=0}^{\infty} \binom{M+2n+1}{2n+1} \xi^{2n+1} [f(2n+1)!]^2 (2n+1)^r \tag{10}$$

where $\hat{a}, \hat{a}^\dagger$ satisfy $[\hat{a}, \hat{a}^\dagger] = 1$.

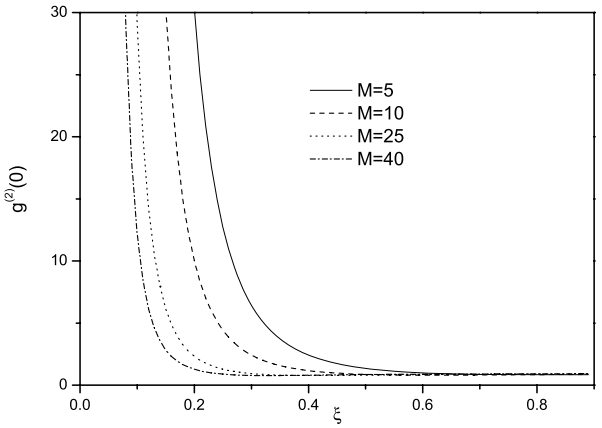

Fig. 1a $g^{(2)}(0)$ for ENLNBS form 1

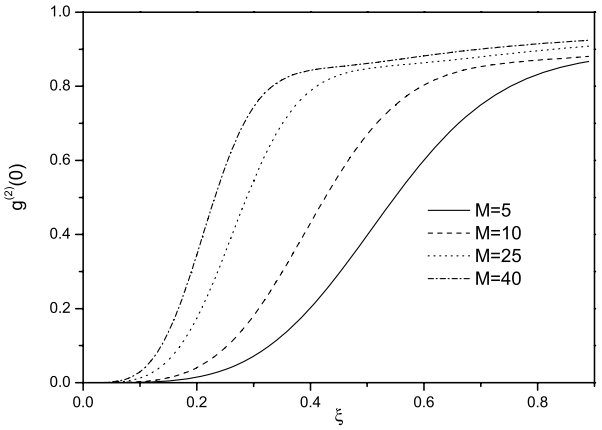

Fig. 1b $g^{(2)}(0)$ for ONLNBS form 1

We make use of the results given by the above equations to calculate the Glauber second order (zero time delay) correlation function which is defined by [1, 2]

$$g^{(2)}(0) = \frac{\langle \hat{a}^{\dagger 2}\hat{a}^2 \rangle}{\langle \hat{a}^{\dagger}\hat{a} \rangle^2} = \frac{\langle \hat{n}^2 \rangle - \langle \hat{n} \rangle}{\langle \hat{n} \rangle^2} \tag{11}$$

The state is said to exhibit super-Poissonian distribution when $g^{(2)}(0) > 1$, Poissonian for $g^{(2)}(0) = 1$ or sub-Poissonian behaviour for $g^{(2)}(0) < 1$ [34]. The auto-correlation function for both the ENLNBS and ONLNBS is investigated numerically. We plot $g^{(2)}(0)$ as a function of ξ for different values of M and η in Figs. 1. It is shown, in Fig. 1a for ENLNBS with form 1, that the distribution starts super-Poissonian for all values of M. But as ξ increases it becomes Poissonian. Further increase in ξ the state becomes sub-Poissonian. For ONLNBS with form 1, (Fig. 1b), the state starts sub-Poissonian for all values of M. For the range considered in the plot the state is still sub-Poissonian. In the other hand, for the ENLNBS with form 2, Figs. 1c, 1d, the state starts super-Poissonian and the distribution oscillates once. The peak appears at lower values of ξ for fixed $\eta(M)$ and increased $M(\eta)$. But for the ONLNBS with the same form 2, Figs. 1e, 1f, the state starts sub-Poissonian and shoots to

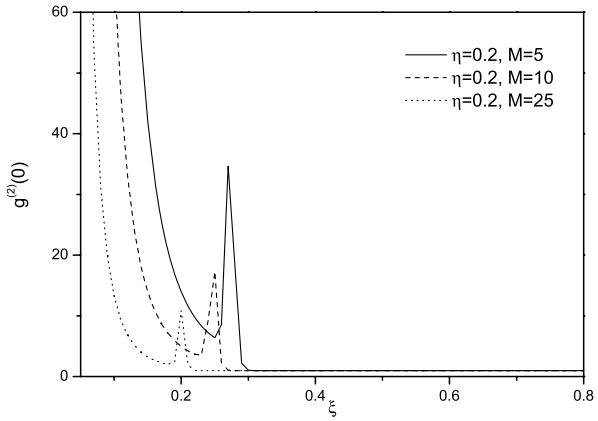

Fig. 1c $g^{(2)}(0)$ for ENLNBS form 2

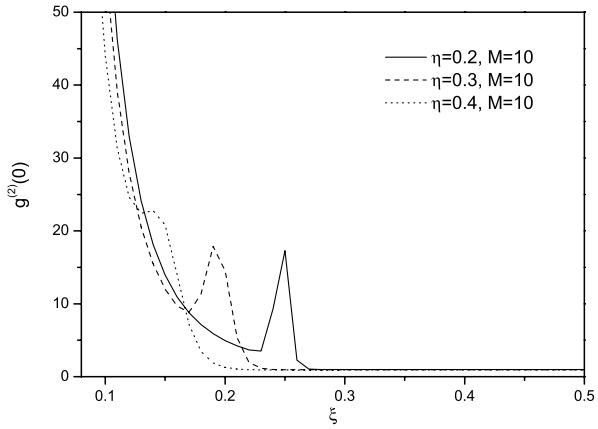

Fig. 1d $g^{(2)}(0)$ for ENLNBS form 2

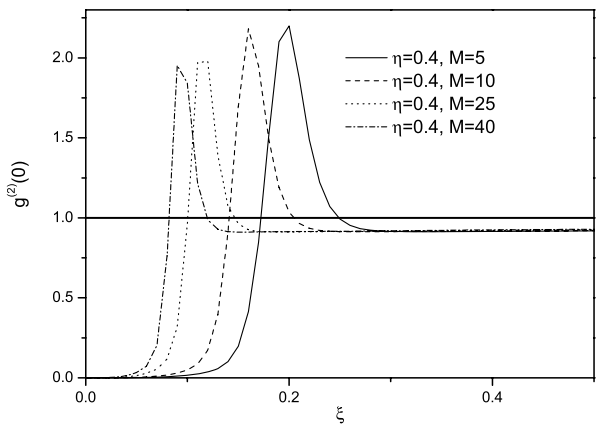

Fig. 1e $g^{(2)}(0)$ for ONLNBS form 2

super-Poissonian, but as ξ increases it settles to sub-Poissonian distribution. The shooting appears at lower ξ for fixed $M(\eta)$ and increased values of $\eta(M)$.

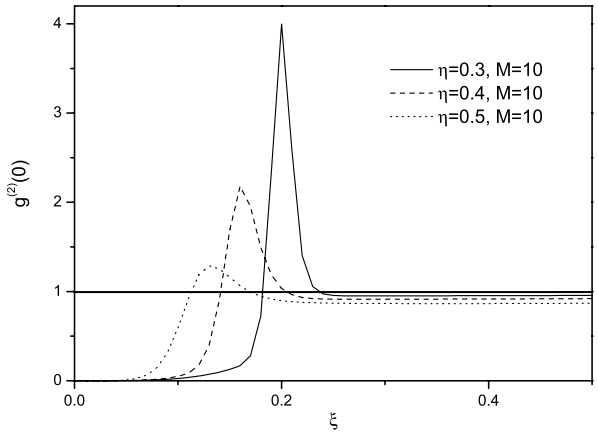

Fig. 1f $g^{(2)}(0)$ for ONLNBS form 2

3.2 Squeezing Effects

3.2.1 Normal Squeezing

It is well known that the squeezed state has less noise than the vacuum state in one of the field quadratures. Therefore, it would be interesting to discuss the phenomenon of squeezing related to the present states. The squeezing parameters depend on the expectation values of the operator $(\hat{a}^r)$. From (3), the expectation values of the operators $\hat{a}^r$ of the present states is obtained as

(i) for ENLNBS

$$\langle \hat{a}^r \rangle_e = |\lambda|_e^2 \sum_{n=0}^{\infty} \binom{M+2n}{2n}^{\frac{1}{2}} \xi^{2n} (f(2n))! \times \binom{M+2n+r}{2n+r}^{\frac{1}{2}} \xi^{2n+r} [f(2n+r)]! \sqrt{\frac{(2n+r)!}{2n!}} \tag{12}$$

It has zero value for odd r.

(ii) for ONLNBS

$$\langle \hat{a}^r \rangle_o = |\lambda|_o^2 \sum_{n=0}^{\infty} \binom{M+2n+1}{2n+1}^{\frac{1}{2}} \xi^{2n+1} [f(2n+1)]! \times \binom{M+2n+1+r}{2n+1+r}^{\frac{1}{2}} \xi^{2n+1+r} (f(2n+1+r))! \sqrt{\frac{(2n+1+r)!}{(2n+1)!}} \tag{13}$$

Again the expectation value for any odd power of $\hat{a}$ is zero. The investigation of normal squeezing (NS) is based on defining two field quadrature operators $\hat{x}$ (coordinate) and $\hat{p}$ (momentum)

$$\hat{x} = \frac{1}{2}(\hat{a} + \hat{a}^{\dagger}) \tag{14}$$

$$\hat{p} = \frac{1}{2i}(\hat{a} - \hat{a}^{\dagger}) \tag{15}$$

These two quadratures are satisfying the commutation relation

$$[\hat{x}, \hat{p}] = \frac{i}{2} \tag{16}$$

Therefore the uncertainty relation to $\hat{x}$ and $\hat{p}$ is

$$(\Delta\hat{x})^2(\Delta\hat{p})^2 \geq 1/16 \tag{17}$$

where $(\Delta\hat{x})^2$ and $(\Delta\hat{p})^2$ are the variances which are defined for any state as

$$(\Delta\hat{x})^2 = \langle\hat{x}^2\rangle - \langle\hat{x}\rangle^2 \tag{18}$$

$$(\Delta\hat{p})^2 = \langle\hat{p}^2\rangle - \langle\hat{p}\rangle^2 \tag{19}$$

and the field is said to be squeezed if $(\Delta\hat{x})^2$ or $(\Delta\hat{p})^2 \leq \frac{1}{4}$.

In the present case $\langle\hat{a}\rangle$ and $\langle\hat{a}^2\rangle$ are real. Thus, the variances of $\hat{x}$ and $\hat{p}$ are

$$(\Delta\hat{x})^2 = \frac{1}{4} + \frac{1}{2}\big(\langle\hat{a}^\dagger\hat{a}\rangle + \langle\hat{a}^2\rangle\big) \quad \text{or} \quad (\Delta\hat{p})^2 = \frac{1}{4} + \frac{1}{2}\big(\langle\hat{a}^\dagger\hat{a}\rangle - \langle\hat{a}^2\rangle\big) \tag{20}$$

Due to the definitions of ENLNBS and ONLNBS it is mentioned that $\langle\hat{a}\rangle = 0$. From the numerical calculations as well as quick arithmetics show that no normal squeezing is apparent. That is there will be no squeezing in the x-quadrature while the p-quadrature squeezing occurs.

3.2.2 Amplitude Squared Squeezing (ASS)

Now we use the concept of ASS introduced by Hillery [35]. This type of squeezing arises in a natural way in second-harmonic generation and in a number of non-linear optical processes. When we study ASS for the present states, our problem may be treated by introducing the field quadrature operators

$$\hat{Y}_0 = \frac{1}{4}\big(\hat{a}\hat{a}^\dagger + \hat{a}^\dagger\hat{a}\big) \tag{21a}$$

$$\hat{Y}_1 = \frac{1}{4}\big(\hat{a}^2 + \hat{a}^{\dagger 2}\big) \tag{21b}$$

$$\hat{Y}_2 = \frac{1}{4}\big(\hat{a}^2 - \hat{a}^{\dagger 2}\big) \tag{21c}$$

Operators $\hat{Y}_1$ and $\hat{Y}_2$ satisfy the commutation relation

$$[\hat{Y}_1, \hat{Y}_2] = i\hat{Y}_0 \tag{22}$$

So that the uncertainty principle applied to $\hat{Y}_1$ and $\hat{Y}_2$ is

$$(\Delta\hat{Y}_1)^2(\Delta\hat{Y}_2)^2 \geq \frac{1}{4}|\langle\hat{Y}_0\rangle|^2 \tag{23}$$

ASS holds if

$$\begin{aligned} d_1 &= (\Delta\hat{Y}_1)^2 - \frac{1}{2}\langle\hat{Y}_0\rangle < 0 \\ &= \langle\hat{a}^4\rangle + \langle\hat{n}^2\rangle - \langle\hat{n}\rangle \end{aligned} \tag{24a}$$

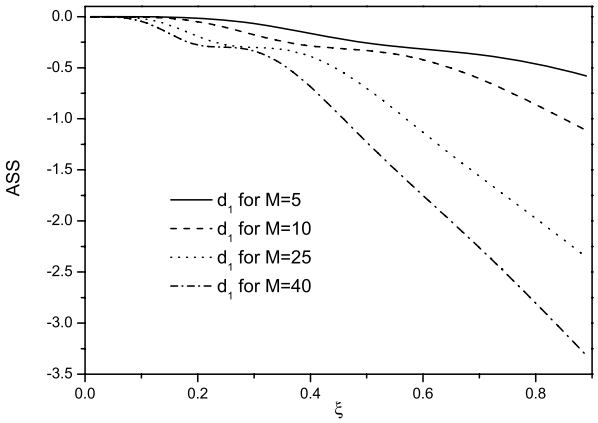

Fig. 2a ASS for ENLNBS form 1

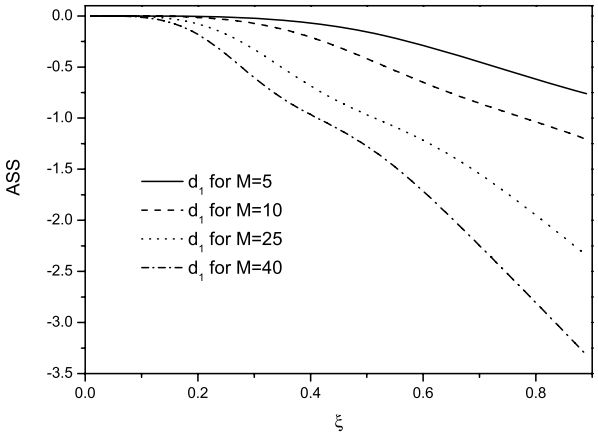

Fig. 2b ASS for ONLNBS form 1

or

$$d_2 = (\Delta \hat{Y}_2)^2 - \frac{1}{2}\langle \hat{Y}_0 \rangle < 0$$
$$= \langle \hat{n}^2 \rangle - \langle \hat{n} \rangle - \langle \hat{a}^4 \rangle \tag{24b}$$

From the above equations with (3) and (5), we have investigated ASS for the ENLNBS and ONLNBS. Now (d_1) and (d_2) (which represent the ASS) is computed and the results are presented in Figs. 2. In these figures, ASS are plotted against the parameter ξ, for the present states. In Figs. 2a, 2b, the ASS occurs in the quadrature (d_1) for values of $\xi > 0$. Increasing M and ξ increases the amount of ASS. On the other hand the quadrature (d_2) shows no squeezing. The effect of the parameter η in form 2 is shown in Figs. 2d, 2f for ENLNBS and ONLNBS. In these figures, squeezing occur for small values of ξ. Increasing η decreases the amount of ASS. Also, the effect of the parameter M is shown in Figs. 2c, 2e. We can show that the ASS for the present states is too sensitive to any variation in the value of the parameter M.

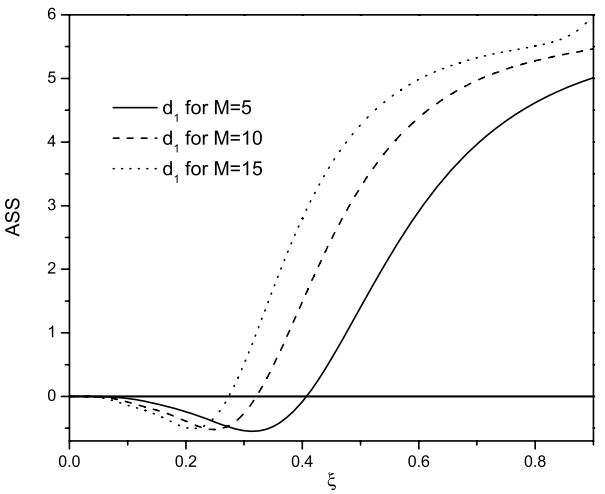

Fig. 2c ASS for ENLNBS for $\eta = 0.7$ form 2

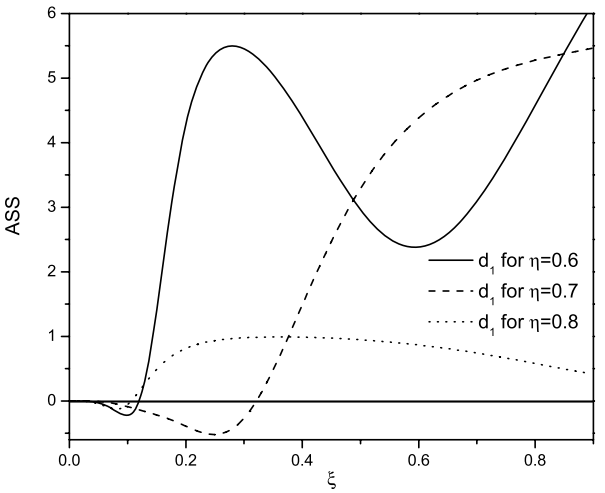

Fig. 2d ASS for ENLNBS for $M = 10$ form 2

3.3 Quasi-Probability Distribution Functions

For the statistical description of a microscopic system and to provide insight into the non-classical features of radiation fields, the quasi-probability distribution functions [36–39] are needed to be studied. These functions are P-representation, Wigner-function (W-function) and Q-functions.

We shall concentrate on the Q-function and W-function only. To find the Q-function, we shall use the definition for the coherent state $|\alpha\rangle$ in the form

$$|\alpha\rangle = \exp\left(-\frac{1}{2}|\alpha|^2\right) \sum_{\ell=0}^{\infty} \frac{\alpha^\ell}{\sqrt{\ell!}} |\ell\rangle \tag{25}$$

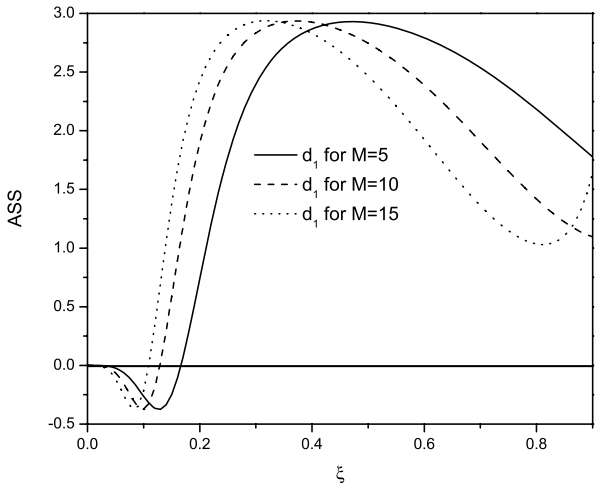

Fig. 2e ASS for ONLNBS for $\eta = 0.7$ form 2

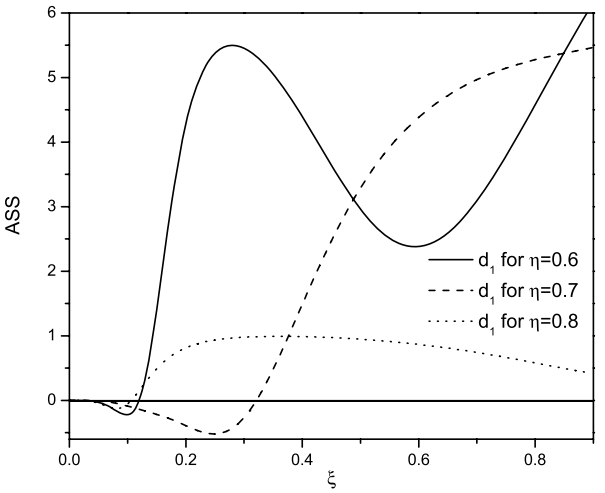

Fig. 2f ASS for ONLNBS for $M = 10$ form 2

then Q-function is defined as

$$Q(\alpha) = \pi^{-1}\langle\alpha|\hat{\rho}|\alpha\rangle \tag{26}$$

where $\hat{\rho}$ is the density matrix. Q-function is calculated for the ENLNBS and ONLNBS in the following

(i) for even NLNBS

$$Q_e(\alpha) = \pi^{-1}|\lambda_e|^2 \exp\bigl(-|\alpha|^2\bigr)|G_e|^2 \tag{27}$$

where

$$G_e = \sum_{n=0}^{\infty} \binom{M+2n}{2n}^{\frac{1}{2}} \xi^{2n} (f(2n))! \frac{(\alpha^*)^{2n}}{(2n)!}$$

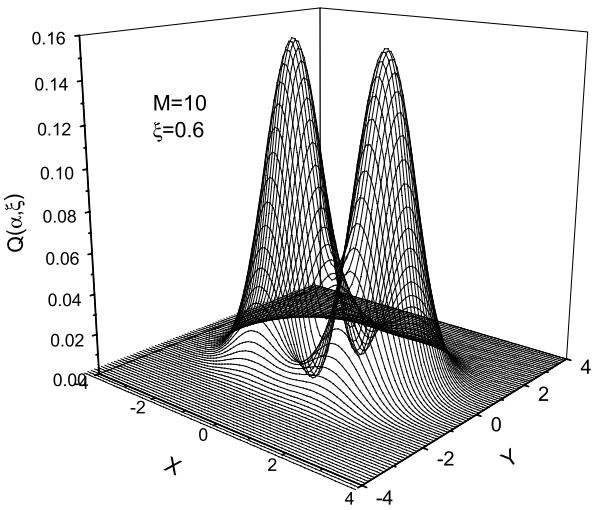

Fig. 3a Q-function for ENLNBS form 1

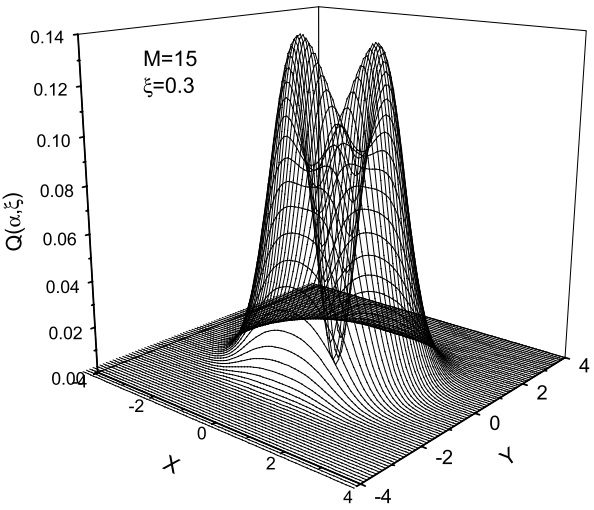

Fig. 3b Q-function for ONLNBS form 1

(ii) for odd NLNBS

$$Q_o(\alpha) = \pi^{-1}|\lambda_o|^2 \exp\left(-|\alpha|^2\right)|G_o|^2 \tag{28}$$

where

$$G_o = \sum_{n=0}^{\infty} \binom{M+2n+1}{2n+1}^{\frac{1}{2}} \xi^{2n+1}[f(2n+1)]! \frac{(\alpha^*)^{2n+1}}{(2n+1)!}$$

with $\alpha = x + iy$.

Curves depicting the Q-function for the ENLNBS and ONLNBS are found in Figs. 3. For form 1, splitting of the one peak structure for the nonlinear NBS [19] into two peaks with interference pattern and squeezing are apparent for ENLNBS for $M = 10$, $\xi = 0.6$

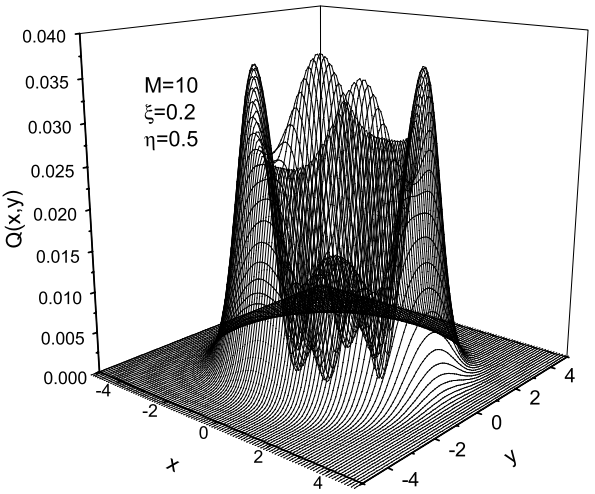

Fig. 3c Q-function for ENLNBS form 2

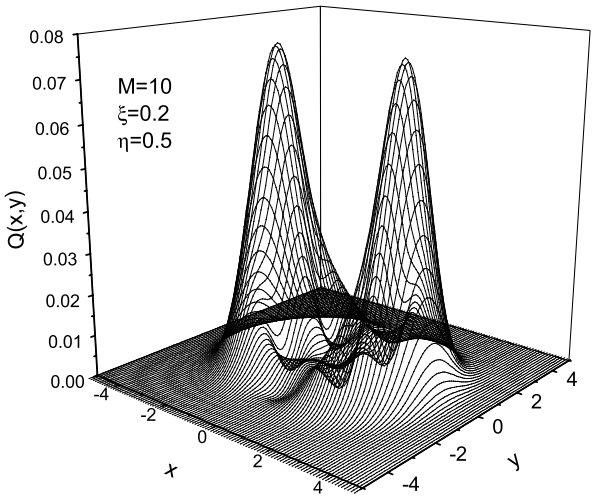

Fig. 3d Q-function for ONLNBS form 2

(Fig. 3a) and ONLNBS for $M = 10$, $\xi = 0.6$ (Fig. 3b). The effect of the parameter η of form 2 in the structure of the Q-function is shown in Figs. 3c, 3d for the ENLNBS and ONLNBS respectively. When we take $M = 10$, $\xi = 0.2$ and $\eta = 0.5$, the ONLNBS shows a two-peak squeezed structure with pattern of interference. While the ENLNBS a four-peak structure with two peaks slightly lower is shown. Also interference structure is apparent there in Fig. 3d.

However, W-function can take negative values for some states and this is regarded as reflection of nonclassical effects. The W-function ($W(\alpha)$) with the off-diagonal terms taken into account in the case of the present states is defined as follows

(i) for ENLNBS

$$W(\alpha) = \frac{2}{\pi}\exp\bigl(-2|\alpha|^2\bigr)|\lambda_e|^2\left[\sum_{n=0}^{\infty}\binom{M+2n}{2n}\xi^{2n}\bigl[\bigl(f(2n)\bigr)!\bigr]^2 L_{2n}^{0}\bigl(4|\alpha|^2\bigr)\right.$$

$$+\sum_{r=1}^{\infty}\sum_{n=0}^{r-1}\binom{M+2n}{2n}^{\frac{1}{2}}\xi^{2n}(f(2n))!\binom{M+2r}{2r}^{\frac{1}{2}}\xi^{2r}(f(2r))!$$
$$\times\sqrt{\frac{(2n)!}{(2r)!}}L_{2n}^{2(r-n)}\big(4|\alpha|^2\big)\big[(2\alpha^*)^{2(r+n)}+(2\alpha)^{2(r-n)}\big]\Bigg] \tag{29}$$

where $L_n^m(4|\alpha|^2)$ is the associated Laguerre polynomial.

The function $L_r(x)$ in (29) is the Laguerre polynomial defined as

$$L_r^0(x)=\sum_{m=0}^{r}(-1)^m\frac{(r)!(x)^m}{(m!)^2(r-m)!}$$

(ii) for ONLNBS

$$W(\alpha)=-\frac{2}{\pi}\exp\big(-2|\alpha|^2\big)|\lambda_o|^2\Bigg[\sum_{n=0}^{\infty}\binom{M+2n+1}{2n+1}\xi^{2n+1}$$
$$\times\big[\big(f(2n+1)\big)!\big]^2L_{2n}^0\big(4|\alpha|^2\big)+\sum_{r=1}^{\infty}\sum_{n=0}^{r-1}\binom{M+2n+1}{2n+1}^{\frac{1}{2}}\xi^{2n+1}$$
$$\times\big(f(2n+1)\big)!\binom{M+2r+1}{2r+1}^{\frac{1}{2}}\xi^{2r+1}\big(f(2r+1)\big)!\sqrt{\frac{(2n+1)!}{(2r+1)!}}$$
$$\times L_{2n+1}^{2(r-n)}\big(4|\alpha|^2\big)\big[(2\alpha^*)^{2(r+n)+2}+(2\alpha)^{2(r-n)}\big]\Bigg] \tag{30}$$

In Figs. 4 we have plotted the W-function for different values of M,ξ and η. Non-classical effects can be studied by measuring the negative values of the W-function. These non-classical effects are exhibited in these figs. of the W-function for the present states. Due to the appearance of the even Fock states only in the ENLNBS, we expect the central peak to point upward for the W-function. This is exhibited in Figs. 4a, 4b (form 1). However as ξ increases a number of other peaks appears besides the central peak. Negative values are attained by the W-function which is a signature of non classically of the state. On the other hand, the W-function for the ONLNBS exhibits a central peak pointing downward as shown in Figs. 4c, 4d (form 1). As ξ increases other rims appear around the central peak. This is due to the fact that the ONLNBS is composed of odd Fock states only. The effect of the parameter η in form 2, is shown in Figs. 4e, 4f for ENLNBS and ONLNBS respectively. The η parameter adds structure to the interference pattern around the central peak where for the ENLNBS and ONLNBS as shown in Figs. 4e, 4f for the case of $\eta=0.5$ while $M=10$ and $\xi=0.2$. Interference pattern is quite pronounced in this case. The effect of the form of the nonlinearity is shown clearly in these figures when compared with the figures for the ENBS and ONBS as discussed in Ref. [40].

3.4 Phase Distribution

The notion of the phase in quantum optics has found renewed interest because of the existence of phase-dependent quantum noise. In this section, the phase properties using the

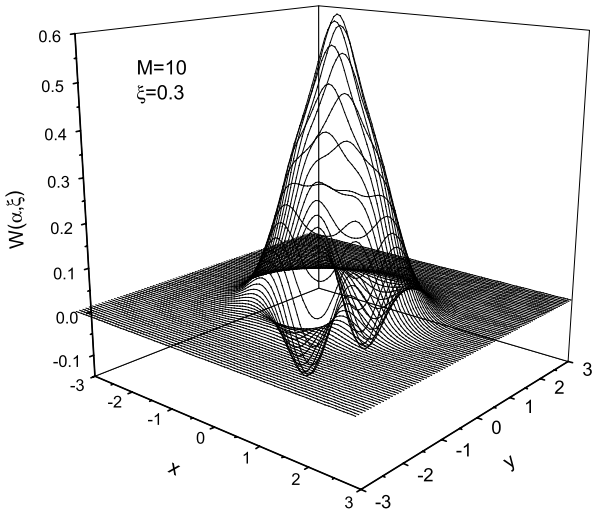

Fig. 4a Wigner function for ENLNBS form 1

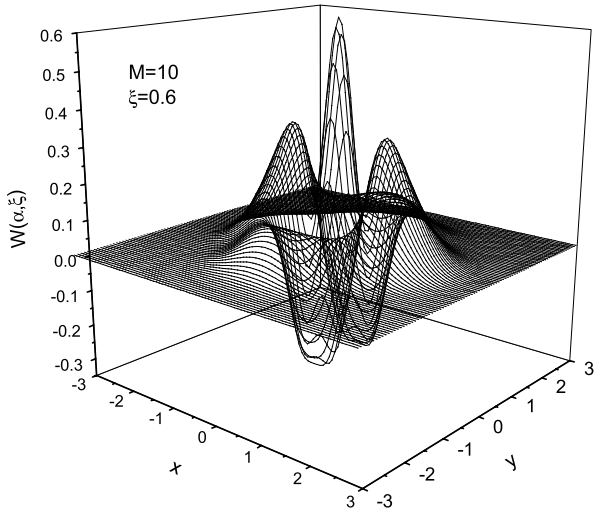

Fig. 4b Wigner function for ENLNBS form 1

Pegg-Barnett method [41, 42] are studied. This method is based on the phase states $|\Theta_m\rangle$, which are defined as

$$|\Theta_m\rangle = \frac{1}{\sqrt{s+1}} \sum_{n=0}^{s} \exp(in\theta_m)|n\rangle \tag{31}$$

where

$$\theta_m = \theta_0 + \frac{2\pi m}{s+1}, \quad m = 0, 1, \ldots, s \tag{32}$$

the value of θ_0 is arbitrary. The set $\{|\Theta_m\rangle\}$ indicates a specific bases set of $(s+1)$ mutually orthogonal phase states. In fact the phase states $|\Theta_m\rangle$ are eigenstates of the Hermitian phase

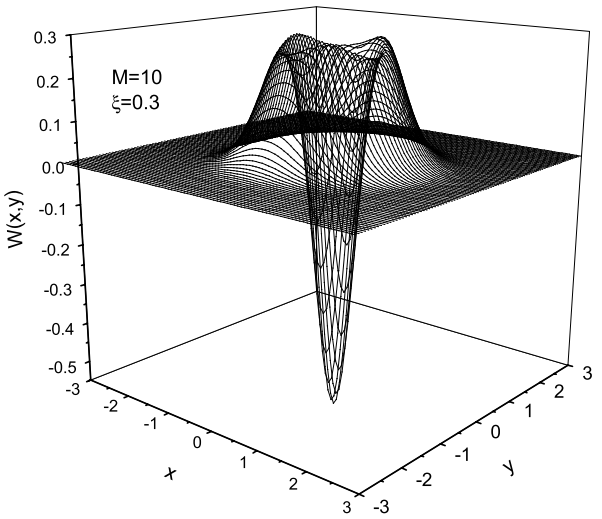

Fig. 4c Wigner function for ONLNBS form 1

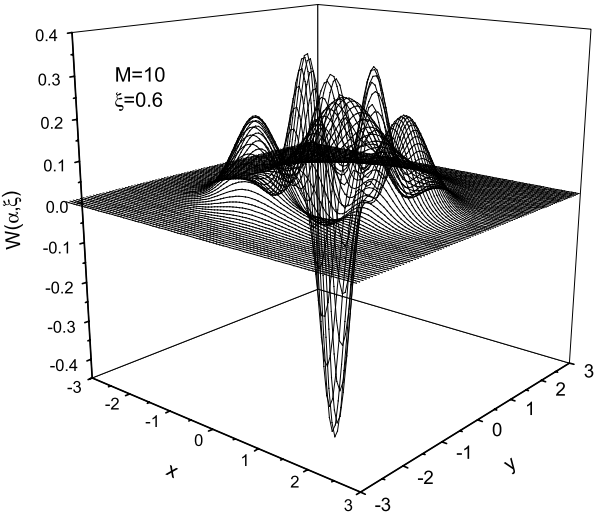

Fig. 4d Wigner function for ONLNBS form 1

operator $\hat{\Phi}_\theta$ given by

$$\hat{\Phi}_\theta = \sum_{m=0}^{s} \theta_m |\Theta_m\rangle\langle\Theta_m| \tag{33}$$

The expectation values are calculated in the finite dimensional space and after that the limit $s \to \infty$ is taken. The state of the form

$$|b\rangle = \sum_{n=0}^{s} b_n e^{in\Psi} |n\rangle \tag{34}$$

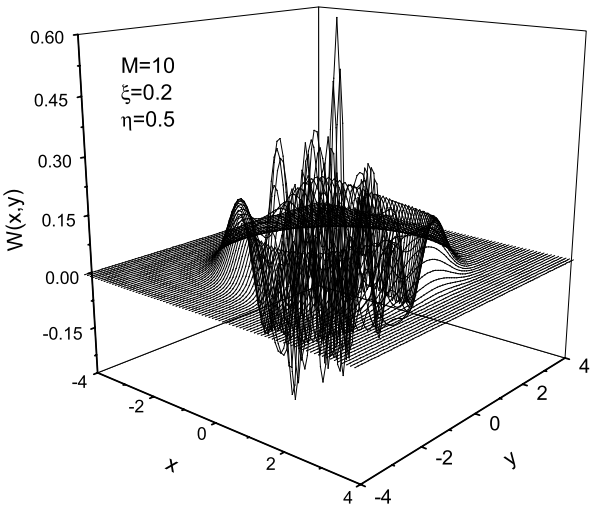

Fig. 4e Wigner function for ENLNBS form 2

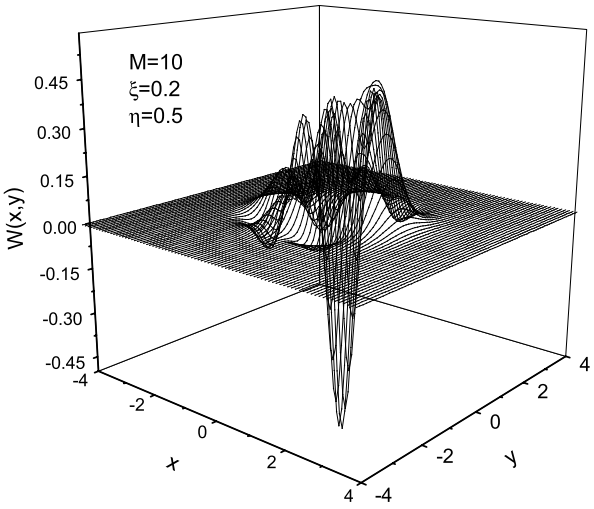

Fig. 4f Wigner function for ONLNBS form 2

is called a partial phase state [31], where b_n are real and positive and Ψ is a phase. From (31) and (34), one can calculate the expectation values of the phase operator and its moments. However, we shall concentrate on the phase probability distribution. This distribution for the partial phase state of (34) is given by

$$\mathrm{Ph}(\theta) = |\langle \Theta_m | b \rangle|^2 \tag{35}$$

Since the density of phase states is $\frac{s+1}{2\pi}$, thus in the continuum limit $s \to \infty$, (35) reduces to

$$\mathrm{Ph}(\xi, \theta) = \frac{1}{2\pi}\left[1 + 2\sum_{n>m}\sum_{m} b_m b_n \cos[(n-m)\theta]\right] \tag{36}$$

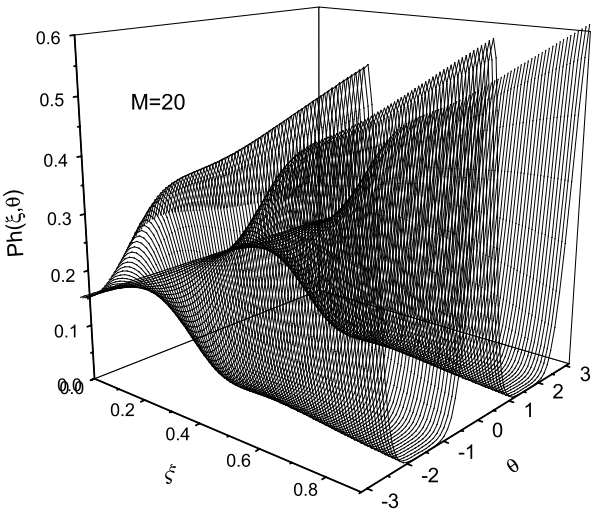

Fig. 5a Phase distribution for ENLNBS form 1

In what follows one calculates this function for the ENLNBS and ONLNBS given by (3) and (5). It is found to be

(i) for ENLNBS

$$\mathrm{Ph}(\xi,\theta)=\frac{1}{2\pi}\Bigg(1+2|\lambda_e|^2\sum_{r=1}^{\infty}\sum_{s=0}^{r-1}\binom{M+2s}{2s}^{\frac{1}{2}}\xi^{2s}[f(2s)]!\times\binom{M+2r}{2r}^{\frac{1}{2}}\xi^{2r}[f(2r)]!\cos[2(r-s)\theta]\Bigg) \tag{37}$$

(ii) for ONLNBS

$$\mathrm{Ph}(\xi,\theta)=\frac{1}{2\pi}\Bigg(1+2|\lambda_o|^2\sum_{r=1}^{\infty}\sum_{s=0}^{r-1}\binom{M+2s+1}{2s+1}^{\frac{1}{2}}\xi^{2s+1}[f(2s+1)]!\times\binom{M+2r+1}{2r+1}^{\frac{1}{2}}\xi^{2r+1}[f(2r+1)]!\cos[2(r-s)\theta]\Bigg) \tag{38}$$

In Figs. 5, the Pegg-Barnett phase distribution $\mathrm{Ph}(\xi,\theta)$ given by (37), (38) is plotted against the parameters ξ and θ, for different values of M,η. In Fig. 5a, the distribution starts from the point $\mathrm{Ph}(\xi,\theta)=\frac{1}{2\pi}$ for $\xi=0$. Because at this point the ENLNBS (ONLNBS) contains the state $|0\rangle$ ($|1\rangle$) and hence phase information is lost. But as ξ increases more states are added and the phase starts to build up for $\xi>0.4$ a peak around $\theta=0$ and two wings at $\theta=\pm\pi$ start to develop. The structure is very well exhibited for $\xi=0.7$ and $M=20$. There is not much difference between the two figures for the ENLNBS and ONLNBS. The effect of the parameter η (form 2) is shown in Figs. 5b, 5c for the ENLNBS and ONLNBS. Here we note the difference between the two distributions for the two states. This is due to the behavior of the Laguerre polynomial and their oscillations which effect the shape of the distributions when $\eta=0.5$ and $M=5$.

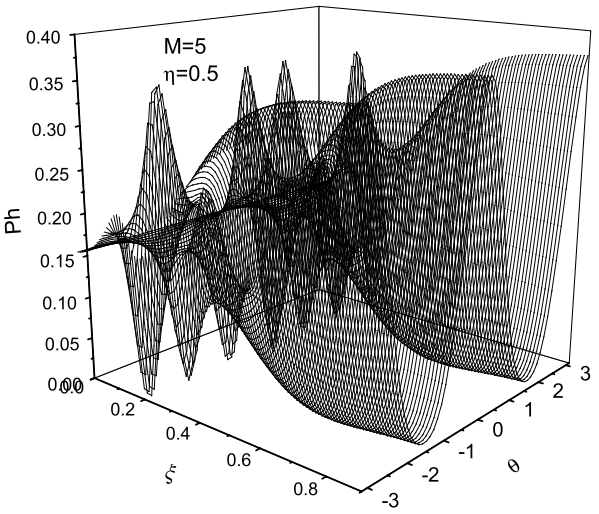

Fig. 5b Phase distribution for even NLNBS state 2

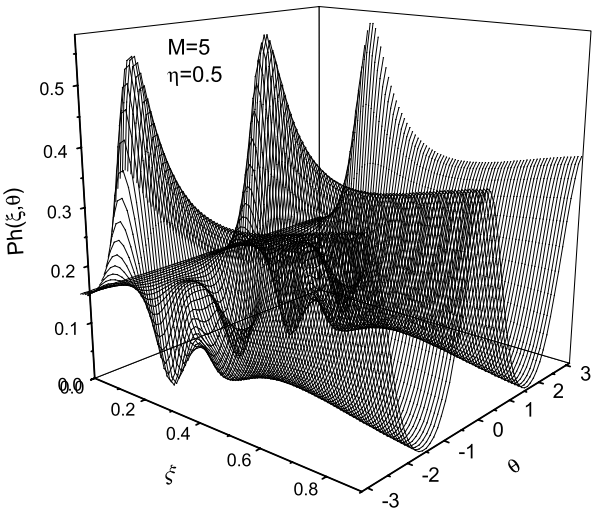

Fig. 5c Phase distribution for ONLNBS form 2

4 Resonance Fluorescence

As an application to the present state we shall consider the resonance fluorescence. In fact the phenomenon of resonance fluorescence provides an interesting manifestation of the quantum theory of light. The phenomenon is related to a radioactively decaying two-level atomic system coupled to an external radiation field in free space. In the steady-state case the mean atomic inversion for a single two-level atom in interaction with an external field at exact resonance is given by [43, 44]

$$\langle \hat{S}(\infty) \rangle_n = -\frac{1}{2} \left(\frac{2\sqrt{2}g}{\gamma \hbar} \right)^{2n} L_n^{(-n-1)} \left(-\frac{\gamma^2 \hbar^2}{8g^2} \right) \tag{39}$$

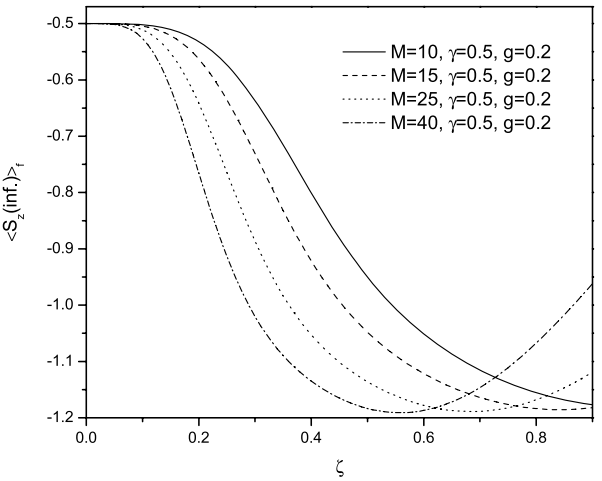

Fig. 6a The atomic inversion for ENLNBS form 1

where γ is the Einstein coefficient, and g is the coupling constant while $L_n^k(x)$ is the generalized Laguerre polynomial. In what follows one calculates the mean atomic inversion for the ENLNBS and ONLNBS given by (3) and (5). It is found to be

(i) for ENLNBS

$$\langle \hat{S}(\infty)\rangle_f = -\frac{1}{2}|\lambda_e|^2 \sum_{n=0}^{\infty}\left(\frac{2\sqrt{2}g}{\gamma\hbar}\right)^{2n}\binom{M+2n}{2n}\xi^{2n} \times \left[(f(2n))!\right]^2 L_n^{(-n-1)}\left(-\frac{\gamma^2\hbar^2}{8g^2}\right) \tag{40}$$

(ii) for ONLNBS

$$\langle \hat{S}(\infty)\rangle_f = -\frac{1}{2}|\lambda_o|^2 \sum_{n=0}^{\infty}\left(\frac{2\sqrt{2}g}{\gamma\hbar}\right)^{2n}\binom{M+2n+1}{2n+1}\xi^{2n+1} \times \left[(f(2n+1))!\right]^2 L_n^{(-n-1)}\left(-\frac{\gamma^2\hbar^2}{8g^2}\right) \tag{41}$$

In Figs 6, we have plotted the atomic inversion for the ENLNBS and ONLNBS given by (40) and (41) against the parameter ξ. For example, in Fig. 6a we have plotted the atomic inversion for ENLNBS (form 1) for different values of the parameter M however, for fixed values of $\gamma = 0.5$ and $g = 0.2$. In this case we observe that the value of the atomic inversion decreases faster as long as we increase the value of M. However, it backs again to increase its value with nearly the same ratio or even faster. For the large values of $M = 30$ or 40, the function reaches its minimum and then changed its direction and starts to increase its value. Changing the direction of the atomic inversion refers to the excitation and de-excitation in the atomic system which would occur during the interaction between the atom and the field. It is quite obvious the function gets nearby the ground state showing de-excitation for large value of M faster than for small value of M provided ξ is small. This means that the atomic inversion is very sensitive to the variation in the parameter M. On the other hand, we have examined the variation of the atomic inversion for fixed value of both $g = 0.2$ and $M = 10$,

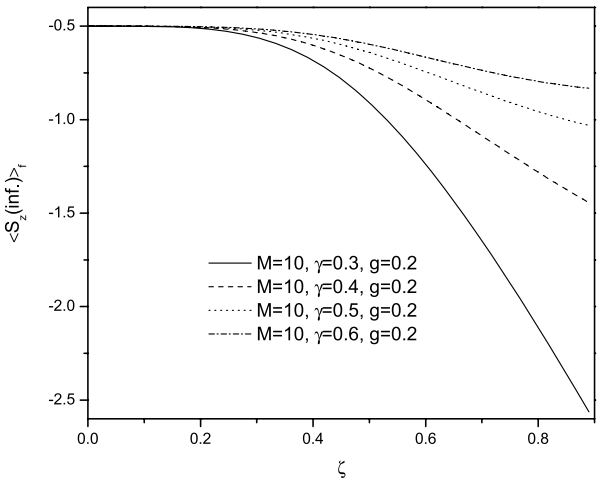

Fig. 6b The atomic inversion for ONLNBS form 1

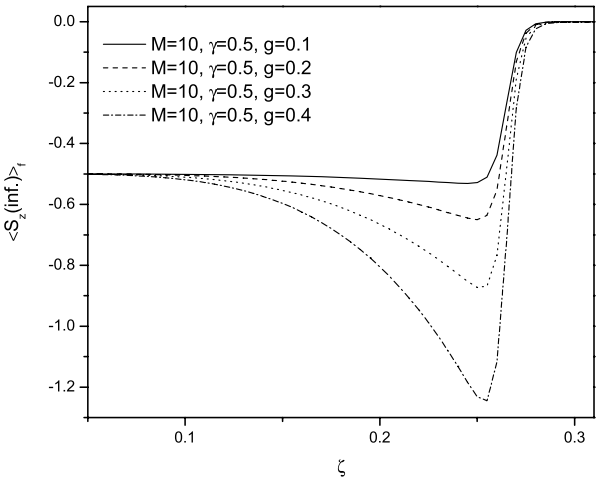

Fig. 6c The atomic inversion for ENLNBS form 2 at $\eta = 0.2$

but with variation in the Einstein coefficient γ. In this case we realize that the function starts to decrease its value with different ratio depends on the value of the parameter γ. However, it backs again to show a slight increment in its value for each case. It should be noted that decreasing in the function value for the case of $\gamma = 0.4$ is significant compare with the other two cases $\gamma = 0.5$, and 0.6 for the case of ONLNBS (form 1), see Fig. 6b. In addition to the effect of the nonlinearity this may due to the existence of the γ factor in the argument of the Laguerre polynomial, (40), (41). To examine the variation in the function resultant of changing the value of the coupling parameter g we have plotted Fig. 6c. In this case we observe that the value of the atomic inversion decreases as we increase the value of g. Also it is noted that the function reaches its minimum at ($\xi \approx 0.255$) and then changed its direction and back again to increase its value, however, it becomes saturated at $zero$ value. As soon as we consider the case in which $g = 0.4$ a dramatic change is occurred in the function behavior where the function shows rapid decreasing in its value. This means that the system gets de-excited where the atom gets nearby to the ground state. Also in Fig. 6d

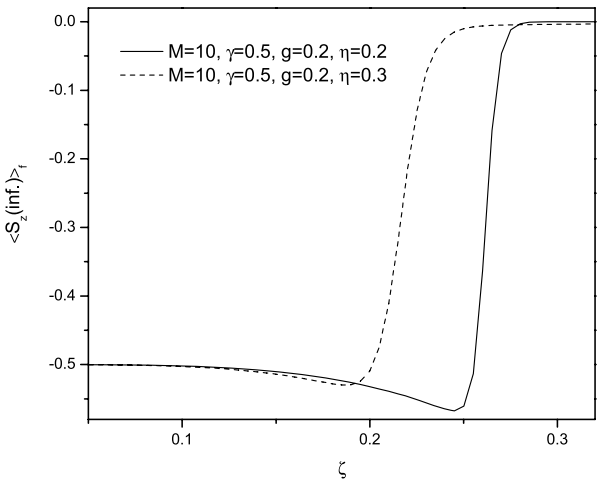

Fig. 6d The atomic inversion for ONLNBS form 2

we can show that the atomic inversion for the present states is too sensitive to any variation in the nonlinearity parameter η. Increasing the value of the parameter η leads to an increase in the atomic inversion value.

5 Conclusion

In this article the ENLNBS and ONLNBS have been introduced and properties of these states are investigated explicitly add: the sub-Poissonian distribution and squeezing. Also the quasi-probability distribution are considered, and non-classical signatures have been exhibited in the W-function. The forms of the nonlinearity functions affect the properties greatly. It has been shown that when we take the nonlinearity form depends on Laguerre polynomials, then the ENLNBS and ONLNBS exhibited different properties especially for the W-function and the phase distribution function. Finally, an application to the resonance fluorescence is given. For a fixed value of the parameter g and the Einstein coefficient γ it has been shown that in a single atom case the excitation in the atomic inversion occurs for large value of both M and γ and the de-excitation occurs for small value of γ, with large value of M.

References

1. Glauber, R.J.: Phys. Rev. **130**, 2529 (1963)
2. Glauber, R.J.: Phys. Rev. **130**, 2766 (1963)
3. Stoler, D., Saleh, B.E.A., Teich, M.C.: Opt. Acta **32**, 345 (1985)
4. Agarwal, G.S.: Phys. Rev. A **45**, 178 (1992)
5. Joshi, A., Lawande, S.V.: J. Mod. Opt. **38**, 2009 (1991)
6. Agrwal, G.S., Inguva, R.: Quantum Optics. Plenum, New York (1991)
7. Simon, R., Satyanarayana, M.V.: J. Mod. Opt. **35**, 719 (1988)
8. Obada, A.-S.F., Hassan, S.S., Puri, R.R., Abdalla, M.S.: Phys. Rev. A **48**, 3174 (1993)
9. Abdalla, M.S., Mahran, M.H., Obada, A.-S.F.: Mod. Opt. **41**, 1889 (1994)
10. Wang, X.G., Fu, H.C.: Int. J. Theor. Phys. **39**, 1437 (2000)
11. Obada, A.-S.F., Abdalla, M.S.: In: Ashour, A.A., Obada, A.-S.F. (eds.) Mathematics and the 21st Century, World Scientific, Singapore (2001), p. 326

12. El-Orany, F.A.A., Mahran, M.H., Obada, A.-S.F., Abdalla, M.S.: Int. J. Theor. Phys. **38**, 1493 (1999)
13. Wineland, D.J., Monroe, C., Itano, W.M., Leibfried, D., King, B.E., Mechhof, D.M.J.: Res. Natl. Inst. Stand. Technol. **103**, 259 (1998)
14. de Matos Filho, R.L., Vogel, W.: Phys. Rev. A **54**, 4560 (1996)
15. Darwish, M.: J. Mod. Opt. **52**(9), 1263 (2005)
16. Mancini, S.: Phys. Lett. A **233**, 291 (1997)
17. Roy, B., Roy., P.: Phys. Lett. A **257**, 264 (1999)
18. Abdalla, M.S., Obada, A.-S.F., Darwish, M.: J. Opt. B: Quantum Semiclass. Opt. **7**, S695 (2005)
19. Abdalla, M.S., Obada, A.-S.F., Darwish, M.: Opt. Commun. **274**, 372 (2007)
20. Obada, A.-S.F., Darwish, M.: J. Mod. Opt. **51**(2), 209 (2004)
21. Obada, A.-S.F., Darwish, M.: J. Opt. B: Quantum Semiclass. Opt. **5**, 211 (2003)
22. Liu, X.M.: J. Phys. A: Math. Gen. **32**, 8685 (1999)
23. Singh, S.: Phys. Rev. A **25**, 3205 (1982)
24. Buck, B., Sukumar, C.V.: Phys. Lett. A **81**, 132 (1981)
25. Sukumar, C.V., Buck, B.: J. Phys. A: Math. Gen. **17**, 877 (1984)
26. Buck, B., Sukumar, C.V.: Phys. Lett. A **83**, 211 (1981)
27. Obada, A.-S.F., Abdel-Hafez, A.M.: Physica A **139**, 593 (1986)
28. Choquette, J.J., Cordes, J.G., Kiang, D.: J. Opt. B: Quantum Semiclass. Opt. **5**, 56 (2003)
29. Roy, B., Roy, P.: J. Opt. B: Quantum Semiclass. Opt. **2**, 65 (2000)
30. Obada, A.-S.F., Darwish, M.: J. Opt. B: Quantum Semiclass. Opt. **7**, 57 (2005)
31. Darwish, M.: Int. J. Mod. Phys. B **4**(19), 715 (2005)
32. de Matos Filho, R.L., Vogel, W.: Phys. Rev. A **54**, 4560 (1996)
33. Vogel, W., de Matos Filho, R.L.: Phys. Rev. A **52**, 4214 (1995)
34. Walls, D.F.: Nature **306**, 141 (1983)
35. Hillery, M.: Phys. Rev. A **40**, 3147 (1989)
36. Wigner, E.: Phys. Rev. **40**, 349 (1932)
37. Wigner, E.: Z. Phys. Chem. B **19**, 203 (1932)
38. Cahill, K.E., Glauber, R.J.: Phys. Rev. **177**, 1882 (1969)
39. Hillery, M., O'Connell, R.F., Scully, M.O., Winger, E.P.: Phys. Rev. **106**, 121 (1984)
40. Joshi, A., Obada, A.-S.F.: J. Phys. A **30**, 8 (1997)
41. Barnett, S.M., Pegg, D.T.: J. Mod. Opt. **36**, 7 (1989)
42. Pegg, D.T., Barnett, S.M.: Phys. Rev. A **39**, 1665 (1989)
43. Hassan, S.S.: Ph.D. Thesis, University of Manchester (1976)
44. Hassan, S.S., Bullough, R.K., Puri, R.R.: Physica A **163**, 625 (1990)